Membranes by the Numbers

Rob Phillips

Abstract Many of the most important processes in cells take place on and across membranes. With the rise of an impressive array of powerful quantitative methods for characterizing these membranes, it is an opportune time to reflect on the structure and function of membranes from the point of view of biological numeracy. To that end, in this chapter, I review the quantitative parameters that characterize the mechanical, electrical, and transport properties of membranes and carry out a number of corresponding order-of-magnitude estimates that help us understand the values of those parameters.

Keywords Membrane properties · Fermi problems · Biological numeracy · Membrane shape

1 The Quantitative Membrane Landscape

The pace at which biology is advancing is staggering. Just as there was a short 50 year gap between the invention of manned flight by the Wright Brothers and the beginning of the space age, in the little more than a half century since the discovery of the structure of DNA and its interpretation through the genetic code, the life sciences have entered their own age, sometimes dubbed "the genome age." But there is more to living matter than genomes. While the genome age has unfolded, a second biological revolution has taken place more quietly. This other success story in the emergence of modern biology is the unprecedented and detailed microscopic view of cellular structures that have been garnered as a result of the emergence of new ways to visualize cells. Both electron and optical microscopy have afforded an incredible view of the cellular interior. In addition, the use of techniques for profiling the molecular contents of cells has provided a detailed, quantitative view of the

R. Phillips (✉)
Department of Applied Physics and Division of Biology and Biological Engineering, California Institute of Technology, Pasadena, CA, USA
e-mail: phillips@pboc.caltech.edu

P. Bassereau, P. Sens (eds.), *Physics of Biological Membranes*,
https://doi.org/10.1007/978-3-030-00630-3_3

proteomes and lipidomes of both cells and the viruses that infect them meaning that, in broad brush strokes, we know both what molecular components the cell is made of and how the cellular interior looks. A particularly fertile example that serves as the backdrop for the present chapter is given by our ever-improving understanding of the membrane organization associated with the organelles and plasma membranes of cells of many kinds [1].

The goal of this chapter is to develop a feeling for membranes in the form of biological numeracy. That is, for the many different ways we can think about membranes whether structurally, mechanically, or electrically, we will try to formulate those insights in quantitative terms. The strategy used here is to move back and forth between a data-based presentation in which key quantitative facts about membranes are examined, and a rule of thumb and simple-estimate mentality, in which we attempt to reason out why those numbers take the values they do. For those cases in which we introduce hard data, our device will be to use the so-called BioNumbers ID (BNID) [2]. Some readers will already be familiar with the PMID (Pubmed ID) that links the vast biological literature and databases. Similarly, the BioNumbers database provides a curated source of key numbers from across biology. By simply typing the relevant BNID into your favorite search engine, you will be directed to the BioNumbers website where both the value of the parameter in question will be reported and a detailed description from the primary literature of how that value was obtained. Unfortunately, my presentation is representative rather than encyclopedic. There is much more that could have (and should have) been said about the fascinating question of membrane numeracy. Nevertheless, the hope is that this gentle introduction will inspire readers to undertake a more scholarly investigation of those topics they find especially interesting, while still providing enough quantitative insights to develop intuition about membranes.

There are many conceivable organizational principles for providing biological numeracy for membranes. The strategy to be adopted here is to organize the numbers that characterize membranes along several key axes, starting with their sizes and shapes, turning then to their chemical makeup, followed in turn by some key themes such as the mechanics of membrane deformations, the transport properties of various molecular species across and within membranes, and the electrical properties of membranes. In particular, depending upon the context, there are many different ways of thinking about membranes (see Fig. 1) and each of these different pictures of a membrane has its own set of characteristic parameters. Once these parameters are in hand, we then attempt to make sense of all of these numbers in a section on membrane Fermi problems with the ambition of this section being to give an order-of-magnitude feeling for the numbers that characterize membranes [3, 4]. The notion of a Fermi problem refers to the penchant of Enrico Fermi to find his way to simple numerical estimates for complex phenomena of all kinds in short order. The chapter closes with a look to the future that lays out my views of some of the key challenges that await the next generation of scientists trying to further the cause of membrane numeracy.

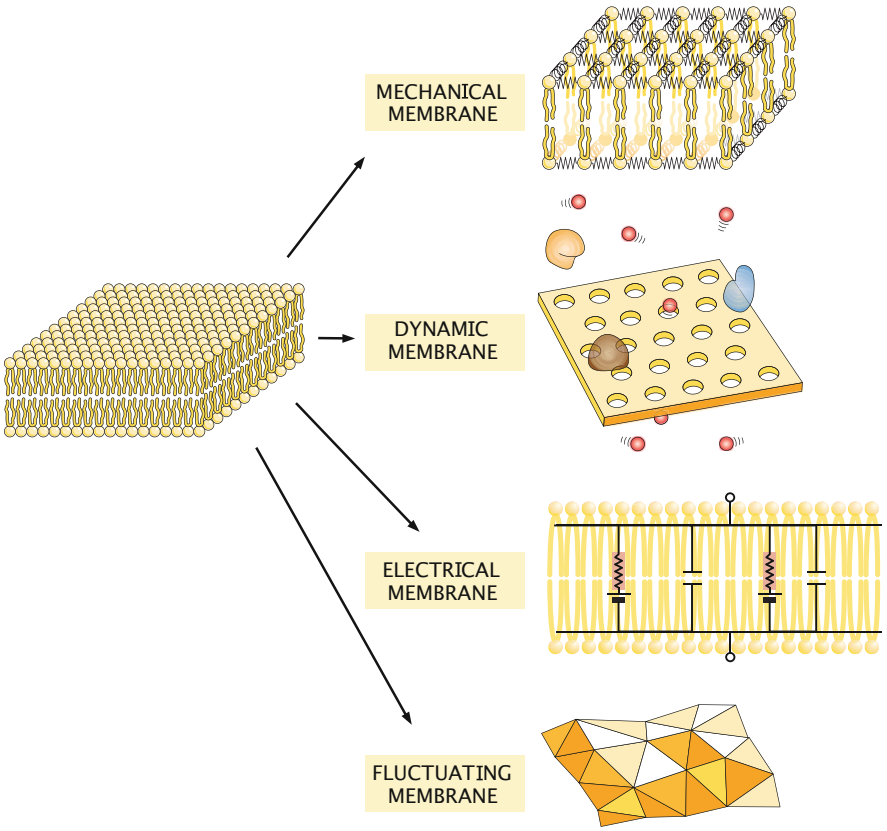

Fig. 1 The many quantitative faces of a membrane. Depending upon the experiments being done or the questions being asked, the way we characterize membranes is different. When thinking about mechanical deformations of a membrane, we will characterize it in terms of elastic constants. Mass transport across and within membranes is described by permeability and diffusion coefficients, respectively. When describing changes in the membrane potential, we characterize the membrane in terms of its conductivity and capacitance. Statistical mechanics teaches us to think about membranes from the standpoint of their fluctuations which interestingly contribute to the membrane tension. Each section of the chapter explores one of these ways of characterizing membranes from the point of view of biological numeracy

2 The Geometrical Membrane: Size and Shape

An inspiring episode from the history of modern science that relates deeply to biological numeracy was the unfolding of our understanding of lipids and the kinds of extended structures they make both in the laboratory and in living cells. In his book "Ben Franklin Stilled the Waves," Charles Tanford gives a charming and insightful tour of this development starting with the efforts of Franklin who was intrigued by the capacity of lipids when spread on water to "still the waves." Indeed,

this fascination led Franklin to a famous experiment in which a spoonful of oil was seen to cover nearly half an acre of Clapham Common near London, giving a first indication of the molecular dimensions of lipids.

Franklin's insights into the structural significance of thin films of lipids led a century later to the emergence of more formal laboratory methods for studying lipid monolayers. In a short 1890 paper on the subject, Lord Rayleigh notes "In view, however, of the great interest which attaches to the determination of molecular magnitudes, the matter seemed well worthy of investigation." To that end, he performed a table-top version of the Franklin experiment concluding that for a film of olive oil he could actually compute the thickness of a monolayer, reporting a lipid length of 1.63 nm [5]. Agnes Pockels in a letter to Lord Rayleigh published in Nature only a year later described her efforts with a trough and force measuring balance to explore surface tension of films on water surfaces [6]. But above all, the study of the "determination of molecular magnitudes" entered a new stage as a result of a tour de force investigation by Irving Langmuir that really gave a first detailed molecular view of lipid molecules and the kinds of collective structures they can form.

Langmuir walks us through his experiments and deep musings about the shape of lipids in his paper entitled "The Constitution and Fundamental Properties of Solids and Liquids. II. Liquids." Here I reproduce a lengthy but interesting series of quotes from that paper, where Langmuir says: "In order to determine the cross-sections and lengths of molecules in oil films, experiments similar to those of Marcelin were undertaken. The oil, or solid fat, was dissolved in freshly distilled benzene, and, by means of a calibrated dropping pipet, one or two drops of the solutions were placed upon a clean water surface in photographic tray. The maximum area covered by the film was measured. Dividing this area by the number of molecules of oil on the surface, the area of water covered by each molecule is readily obtained. The results are given in the first column of Table I." Langmuir's Table I is reproduced here as our own Fig. 2 and shows the impressive outcome of his work, providing not only key numbers but also a much-needed object lesson in the power of indirect experimental methods. He then goes on to tell the reader how he found the lengths of these same molecules noting, "The volume of each molecule is found by dividing the "molecular volume" of the oil (M/ρ) by the Avogadro constant N. By dividing this volume by the cross-section of each molecule, the length of the molecule in a direction perpendicular to the surface can be obtained."

Langmuir then goes on to say: "It is interesting to compare these lengths with the cross-sections. As a rough approximation we may assume that the dimensions of the molecule in directions parallel to the surface can be found by taking the square root of cross-section. This is equivalent to assuming that each molecule in the surface film occupies a volume represented by a square prism with its axis vertical. The length of the square side, which we shall refer to as the average diameter, is given in the second column of Table I, while the height of the prism (or the length of the molecule) is given in the third column." Again, the reader is encouraged to refer to Fig. 2 to see Langmuir's results. He then proceeds telling us "It is seen at once that the molecules are very much elongated. Thus the length of the palmitic

TABLE I.
Preliminary Measurements of Cross-Sections and Lengths of Molecules.

Substance	Formula	I. Cross-section. Sq. cm.	II. $\sqrt{\text{Cross. sec.}}$ Cm.	III. Length. Cm.	IV. Length per carbon atom.
Palmitic acid	$C_{15}H_{31}COOH$	21×10^{-16}	4.6×10^{-8}	24.0×10^{-8}	1.5×10^{-8}
Stearic acid	$C_{17}H_{35}COOH$	22×10^{-16}	4.7×10^{-8}	25.0×10^{-8}	1.39×10^{-8}
Cerotic acid	$C_{25}H_{51}COOH$	25×10^{-16}	5.0×10^{-8}	31.0×10^{-8}	1.20×10^{-8}
Tristearin	$(C_{18}H_{35}O_2)_3C_3H_5$	66×10^{-16}	8.1×10^{-8}	25.0×10^{-8}	1.32×10^{-8}
Oleic acid	$C_{17}H_{33}COOH$	46×10^{-16}	6.8×10^{-8}	11.2×10^{-8}	0.62×10^{-8}
Triolein	$(C_{18}H_{33}O_2)_3C_3H_5$	126×10^{-16}	11.2×10^{-8}	13.0×10^{-8}	0.69×10^{-8}
Trielaidin	$(C_{18}H_{33}O_2)_3C_3H_5$	120×10^{-16}	11.0×10^{-8}	13.6×10^{-8}	0.72×10^{-8}
Cetyl palmitate	$C_{15}H_{31}COOC_{16}H_{33}$	23×10^{-16}	4.8×10^{-8}	41.0×10^{-8}	2.56×10^{-8}
Myricyl alcohol	$C_{30}H_{61}OH$	27×10^{-16}	5.2×10^{-8}	41.0×10^{-8}	2.37×10^{-8}

Fig. 2 Lipid sizes as obtained by Langmuir [7]. This table shows that already a century ago, indirect methods had yielded a quite modern picture of lipid geometry

acid molecule is about 5.2 times the average diameter. The results prove that the molecules arrange themselves on the surface with their long dimension vertical as is required by the theory." [7]. Langmuir went much farther commenting on the significances of the different lengths and areas emboldening him even to think about the role of unsaturated bonds in determining molecular shape. Indeed, one of my favorite aspects of these experiments from Langmuir is that they led him to understand both the number of tails and their degree of saturation truly providing a detailed molecular picture of these molecules. This work went even farther in the hands of Gorter and Grendel who used similar trough experiments to hypothesize that biological membranes are lipid bilayers, a subject we will take up again in the section on "The Electrical Membrane," though I note that there are subtleties about the Gorter and Grendel approach that continue to escape me since in their analysis, they did not account in any way for the fraction of the membrane that is taken up by membrane proteins [8].

What we see from this short historical interlude is that already at the beginning of the twentieth century, long before tools such as X-ray diffraction and nuclear magnetic resonance had made their way onto the scene of modern biological science, scientists had already gleaned a detailed view of the makeup of lipids and started to synthesize a view of how they assemble in cell membranes. The same story already told by experiments using Langmuir troughs has been retold much more accurately on the basis of X-ray and electron microscopy experiments [9, 10]. Indeed, an assessment of the current state of the art for the same kinds of questions originally broached by Langmuir can be seen in Table 1.

The rules of thumb that emerge from a century of study of these molecules is that we should think of lipid masses as being in the range of many hundreds of Daltons up to thousands of Daltons for the largest lipids. The lengths of these lipids vary with tail lengths of ≈2–2.5 nm. The tail-length rule of thumb can be articulated more precisely in terms of the number of carbons in the tail (n_c) as $l_c = n_c l_{cc}$, where the length of a carbon–carbon bond is approximately $l_{cc} \approx 0.13$ nm [11]. The

Table 1 Summary of modern version of measured lipid geometric parameters to be compared to those from Langmuir shown in Fig. 2

Lipid	Area/lipid (nm^2)	Thickness (nm)
DLPE	0.51 ± 0.005	2.58
DOPS	0.65 ± 0.005	3.04
DMPC	0.61 ± 0.005	2.54
DLPC	0.63 ± 0.005	2.09
POPC	0.68 ± 0.015	2.71
diC22:1PC	0.69 ± 0.0005	3.44
DOPC	0.72 ± 0.005	2.68

All values taken from [9]

cross-sectional areas of lipids can be captured by a rule of thumb that the area per lipid is $\approx$0.25–0.75 nm^2. Note that the use of a single cross-sectional area is overly facile because lipids can have much richer shapes than the "square prism with its axis vertical" described by Langmuir. Indeed, because lipids can have shapes more like wedges, this can lead to spontaneous curvature, a topic that we will not delve into more deeply here, but that is critical to understanding the relation between membrane shape and lipid geometry. These rules of thumb are based upon a host of different measurements, with the thickness and area per molecule found here (BNID 101276, 104911, 105298, 105810, 105812). We have traveled a very long way since the days of Langmuir, since we can now order designer lipids with specific chemical properties and even with special groups attached making these lipids fluorescently labeled.

A higher-level view of the structure of cell membranes has been developing on the basis of electron cryo-microscopy which offers an unprecedented view of the very same structural features already explored a century ago using the kinds of indirect methods described above. Figure 3 provides a collage of electron cryo-microscopy images of bacterial cell membranes. We see that in most of these cases, the inner and outer membranes are easily resolved and that they have a thickness of roughly 5 nm (BNID 104911). To be more precise, we should bear in mind that in quoting numbers such as a membrane thickness of 5 nm, of course, we are talking about a characteristic dimension since the interaction of the lipids with the surrounding proteins can induce thickness variations due to the effect of hydrophobic matching of the proteins and lipids [12–14]. Since the bacteria themselves are several microns in length and a bit less than a micron in diameter, we can make a simple estimate of the overall membrane area of the inner and outer membranes by thinking of the bacterium as a spherocylinder with a characteristic volume of 1 $\mu m^3 \approx$ 1 fL and a corresponding surface area of 5–10 μm^2.

The membranes of eukaryotic organisms are typically more heterogeneous and complex than those shown in Fig. 3. Figure 4 gives several examples coming from electron microscopy to make that point. First, such cells, like their prokaryotic counterparts, have an external plasma membrane that separates them from the rest of the world. But as seen in Fig. 4a, even the cell surface can adopt extremely complex geometries as exemplified by the microvilli. One of my favorite examples in all of biology is shown in Fig. 4b where we see the outer segment of a photoreceptor

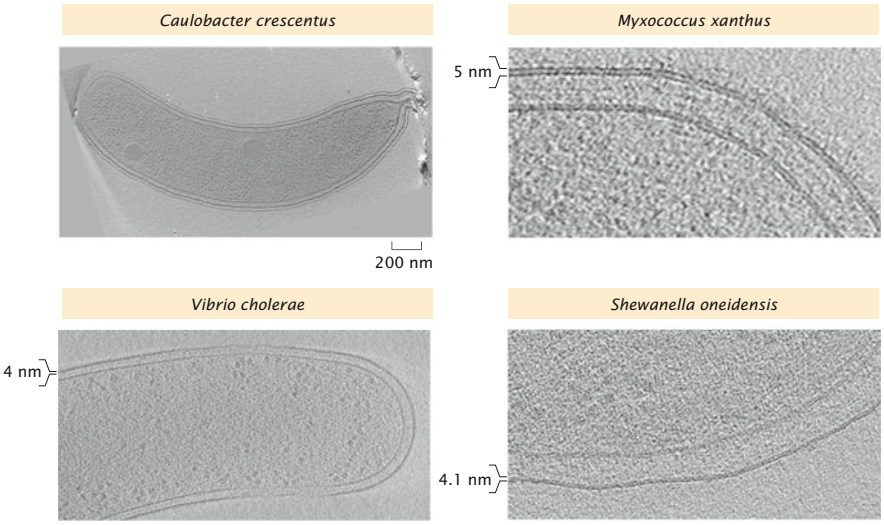

Fig. 3 Electron cryo-microscopy images of bacterial cell walls. The *Caulobacter crescentus* cell gives an impression of overall cell dimensions while the higher-resolution images of other bacteria zoom in on their membranes. Note that these are gram-negative bacteria meaning that their external membrane architecture consists of an inner membrane, a cell wall, and an outer membrane (images courtesy of Grant Jensen and his laboratory members)

with its dense and regular array of membrane stacks. However, it is perhaps the spectacular organellar membranes (see Fig. 4c) that give a sense of the great challenges that remain in understanding membrane shape in cells [15]. Structural complexity similar to that found in the mitochondria abounds in other organelles such as the endoplasmic reticulum [16, 17].

Our brief foray into the size and shape of membranes and the molecules that make them up would of course be woefully incomplete without also commenting briefly on the role proteins play in our modern view of biological membrane structures. Though early ideas about cell membranes painted a picture of a sea of lipids dotted with membrane proteins, the modern view has turned out to be altogether different. "A picture is emerging in which the membrane resembles a cobblestone pavement, with the proteins organized in patches that are surrounded by lipidic rims, rather than icebergs floating in a sea of lipids." [18]. As a rule of thumb, we can think of the protein densities in bacterial membranes as being $\sigma \approx 10^5$ proteins/μm^2. This can be used in turn to estimate the typical center-to-center protein spacing in the cell membrane as $d \approx \sigma^{-\frac{1}{2}} \approx 3\,\text{nm}$, a result that is uncomfortably tight given that typical protein sizes are themselves 3–5 nm as seen in Fig. 5. The question of mean membrane-protein spacing is also of great interest in the context of organellar membranes, with a hint at what can be expected in these cases given by a classic study on synaptic vesicles [18].

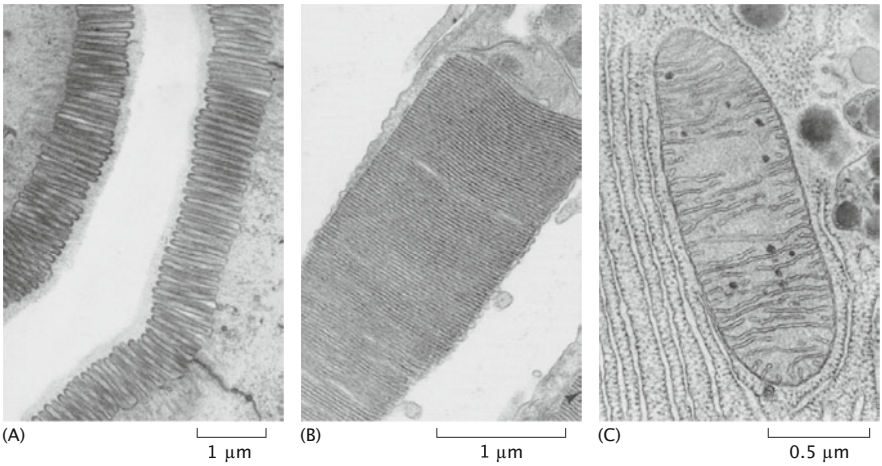

Fig. 4 Eukaryotic membrane structures. (**a**) Apical surface of intestinal epithelial cells showing the dense membrane folds around the microvilli. The sugar chains extending outwards from the surface of the membrane can also be seen as a fuzzy layer above the microvilli. (**b**) Stacks of membranes packed with photoreceptors in the outer segment of a rod cell. (**c**) Thin section of a mitochondrion surrounded by rough endoplasmic reticulum from the pancreas of a bat (all figures adapted from "Physical Biology of the Cell," Garland Press, 2012)

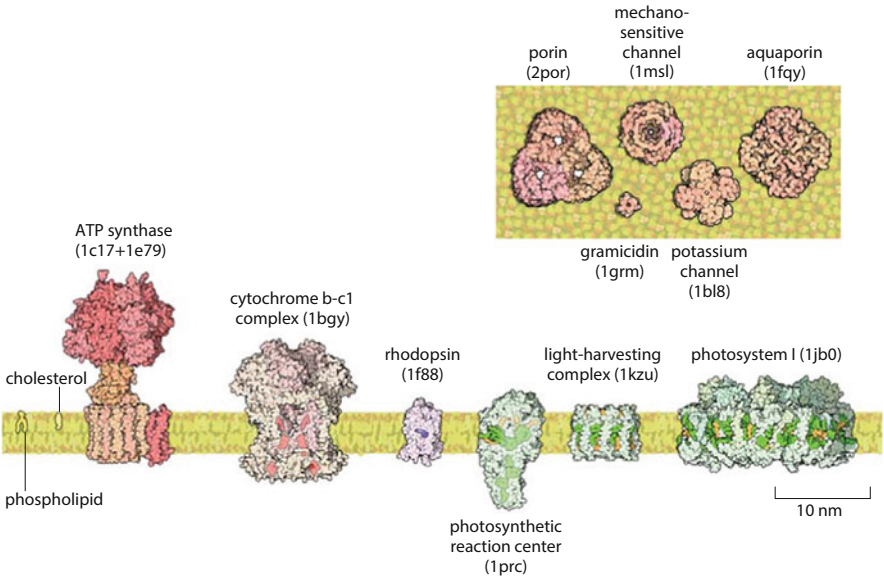

Fig. 5 Sizes and shapes of membrane proteins [19]. Top and side views of several notable membrane proteins. Note the 10 nm scale bar, though the membrane thickness can also be used as a scale marker as indicated in Fig. 3 (images courtesy of David Goodsell and adopted from "Cell Biology by the Numbers", Garland Press, 2015)

3 The Chemical Membrane

With each passing generation, our understanding of the structures of the cell is becoming more and more refined. As shown in the previous section, we have learned a huge amount about the structures of membranes and the molecules that make them up. But what about the specific chemistry of these membranes? One of the ways that our picture of the membranes of living cells has been transformed is through the ability to count up the molecules of different kinds, both the lipids making up the plasma membrane and organelles and of the many proteins that decorate these membranes. In many ways, the development of a census of lipid composition of membranes is an astonishing achievement and has revealed not only that these membranes are heterogeneous, but also that the cell "cares" about its lipid composition [18, 20–28]. Though there is still much left to be understood about precisely how cells keep track of their membrane composition and why they "care," in this section of the chapter we focus on what has been learned thus far about these chemical effects from a quantitative perspective. For a pedagogical review, see chapter 4 of Buehler's interesting book [1].

The same membrane strategy used to separate the interior of cells from the extracellular medium is also used for separating the cellular interior into a collection of membrane-bound organelles such as the nucleus, the endoplasmic reticulum, the Golgi apparatus, and mitochondria. Each of these membrane systems is host to lipids that come in different shapes, sizes, and concentrations. There are hundreds of distinct types of lipid molecules found in these membranes and, interestingly, their composition varies from one organelle to the next. This is highly intriguing since these distinct membrane systems interact directly through intracellular trafficking by vesicles. This same heterogeneity applies to the asymmetric plasma membrane, with different classes of lipids occupying the outer and cytosolic leaflets of the membrane (i.e., the two faces of the lipid bilayer).

Experimentally, the study of lipid diversity is a thorny problem. Sequencing a set of single or double bonds along a carbon backbone requires very different analytic tools than sequencing nucleotides in DNA or amino acids along proteins. Still, the omics revolution has hit the study of lipids too. The use of careful purification methods coupled with mass spectrometry has made inroads into the lipid composition of viral membranes, synaptic vesicles, and organellar and plasma membranes from a number of different cell types. Indeed, the numbers in this section owe their existence in no small measure to the maturing field of lipidomics, based in turn upon impressive advances in mass spectrometry. As noted above, we remain largely in the fact-collection stage of this endeavor since a conceptual framework that allows us to understand in detail the whys and wherefores of lipid compositions and how they change with growth conditions is quite immature.

Perhaps the simplest question we can pose about lipids at the outset is how many there are in a typical cell membrane. A naive estimate for a bacterial cell can be obtained by noting that the area of the bacterial cell membrane is roughly $5\,\mu m^2$, and recalling further that many bacteria have both an inner and outer membrane. To

effect the estimate, we take

$$N_{\text{lipids}} = \frac{4 \times \text{membrane area}}{\text{area per lipid}} \approx \frac{20 \times 10^6 \text{ nm}^2}{1/4 \text{ nm}^2} \approx 8 \times 10^7, \tag{1}$$

where the factor of 4 accounts for the fact that we have two lipid *bilayers* because of the presence of both an inner and outer membrane. This estimate is flawed, however, because we failed to account for the fraction of the membrane area that is taken up by proteins rather than lipids. As was seen in the previous section on size and shape, a useful rule of thumb is that 1/4 of the membrane area is taken up by proteins [20], so our revised estimate of the number of lipids in a cell membrane would be reduced by 25%. Further, note that we used an area per lipid on the low side and if we amended that estimate to a value of $\approx 0.5\,\text{nm}^2$ per lipid, this would also bring our estimate down by a factor of two. Literature values reported for the bacterium *E. coli* claim roughly 2×10^7 lipids per *E. coli* cell, squaring embarrassingly well with our simple estimate, and leaving us with a useful rule of thumb for the lipid density of

$$\sigma \approx \frac{2 \times 10^7 \text{ lipids}}{5\,\mu\text{m}^2 \times 4 \text{ leaflets}} \approx 10^6 \frac{\text{lipids}}{\mu\text{m}^2 \text{ leaflet}}. \tag{2}$$

Given our estimate of 2×10^7 lipids per bacterial cell, we can make a corresponding estimate of the fraction of the cell's dry mass that is lipids [29]. As a basis for comparison, we recall that the number of proteins per bacterial cell is $\approx 3 \times 10^6$ [4, 19, 29]. If these proteins have an average mass of 30,000 Da, this means the total protein mass is roughly 10^{11} Da or 0.15 pg, corresponding to roughly 1/2 of the dry mass of a bacterial cell. For our 2×10^7 lipids, each with a mass of roughly 1000 Da, this means that the lipids contribute an approximate mass of 2×10^{10} Da, corresponding to 20% of the protein mass, or 1/10 of the dry mass of the cell.

What about the composition of membranes? In broad brush strokes, what has been learned in lipidomic studies is that in most mammalian cells, phospholipids account for approximately 60% of total lipids by number and sphingolipids make up another 10%. Non-polar sterol lipids range from 0.1% to 40% depending on cell type and which subcellular compartment is under consideration. The primary tool for such measurements is the mass spectrometer. In the mass spectrometer each molecule is charged and then broken down, such that the masses of its components can be found and from that its overall structure reassembled. Such experiments make it possible to infer both the identities and the number of the different lipid molecules. Absolute quantification is based upon spiking the cellular sample with known amounts of different kinds of lipid standards. One difficulty following these kinds of experiments is the challenge of finding a way to present the data such that it is actually revealing. In particular, in each class of lipids there is wide variety of tail lengths and bond saturations. Figure 6 makes this point by showing the result of a recent detailed study of the phospholipids found in budding yeast. In Fig. 6a, we see the coarse-grained distribution of lipids over the entire class of species of lipids

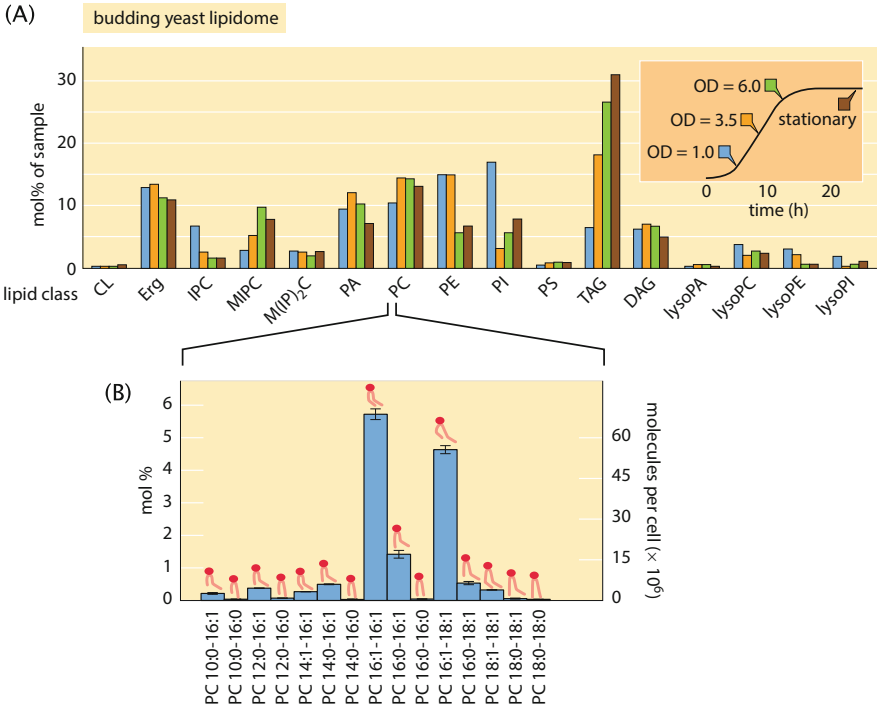

Fig. 6 Lipids in yeast. (**a**) The top panel shows the relative proportions of different types of lipid as a function of the physiological state of the cells as revealed by the inset in the upper right. That inset shows the result of cellular growth as measured by spectrophotometry and leading to the optical density (OD) as a function of time. (**b**) The lower panel shows the diversity of different phospholipids. These lipids exhibit both different tail lengths and degree of saturation as shown by the schematics of the lipids in the lower panel. The abbreviations used in the figure are: *CL* cardiolipin; *Erg* ergosterol; *IPC* inositolphosphorylceramide; *MIPC* mannosyl-inositol phosphorylceramide; *M(IP)2C* mannosyl-di-(inositolphosphoryl) ceramide; *PA* phosphatidic acid; *PC* phosphatidylcholine; *PE* phosphatidyl-ethanolamine; *PI* phosphatidylinositol; *PS* phosphatidylserine; *TAG* triacylglycerols; *DAG* diacylglycerol; *LPC* lysophosphatidylcholine. Adapted from "Cell Biology by the Numbers," Garland Press, 2015. Data in top panel adapted from [27] and data in bottom panel adapted from [22]

found while Fig. 6b gives a more detailed picture of the diversity even within one class of lipids [22]. Studies like the one presented above for yeast have also been done in other eukaryotes as shown in Fig. 7 [21, 30]. Data like this shows that the subject is even more interesting than one might first expect because we see that lipid composition is different for different organelles. As noted earlier, this is especially intriguing given the fact that these different organelles are in dynamical contact as a result of intracellular trafficking, calling for a mechanistic and quantitative description of how these composition heterogeneities are maintained. All of these measurements leave us with much left to understand since as noted at the beginning

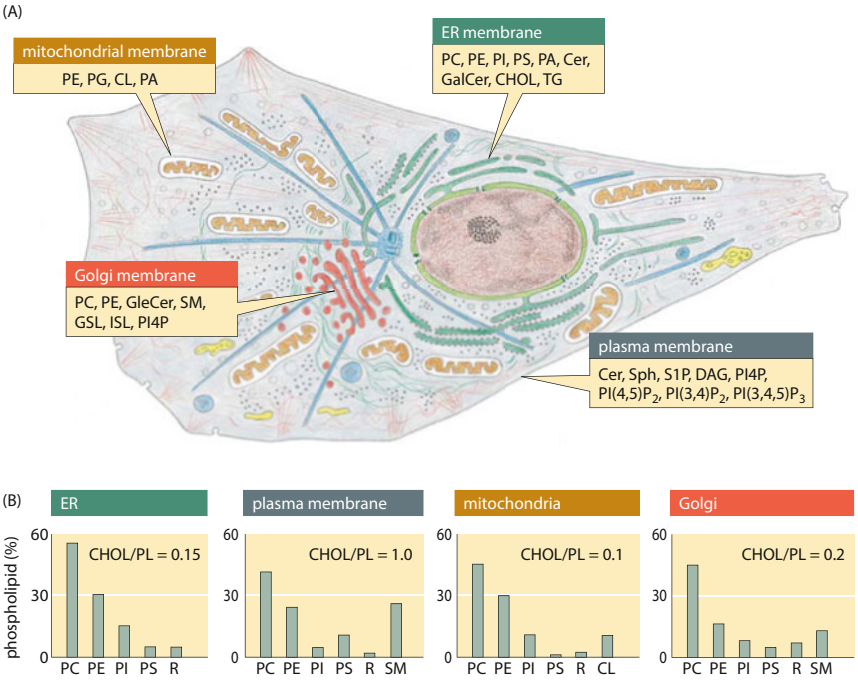

Fig. 7 Organellar lipids in mammalian cells. (**a**) Lipid production is spread across several organelles. The text associated with each organelle shows the site of synthesis for the major lipids. The main organelle for lipid biosynthesis is the endoplasmic reticulum (ER), which produces the bulk of the structural phospholipids and cholesterol. (**b**) The lipid composition of different membranes also varies throughout the cell. The graphs show the composition out of the total phospholipid for each membrane type in a mammalian cell. As a measure of sterol content, the molar ratio of cholesterol to phospholipid is indicated. *SM* sphingomyelin; *R* remaining lipids. For more detailed notation see caption of Fig. 6 (adapted from [21])

of this section, the question of how cells regulate and control their lipid composition and why they care remains unanswered.

4 The Mechanical Membrane

Electron microscopy images make it abundantly clear that whether we think of the stacked membrane discs making up the outer segment of a photoreceptor or the tortuous folds of the endoplasmic reticulum of a pancreatic cell, biological membranes are often severely deformed. But as we all know from everyday experience, changing the shape of materials usually costs energy. As a result of membrane deformations, energetic costs resulting from both membrane stretching and bending are incurred. The aim of this part of the chapter is to give a quantitative

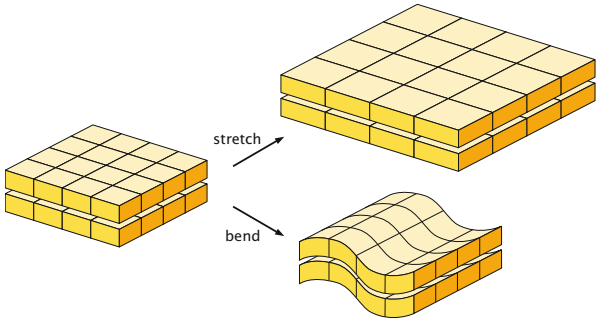

Fig. 8 The mechanics of membrane deformations. One of the deformation modes is changing the membrane area by stretching. The second mode of membrane deformation considered here is membrane bending

view of the energetic cost of these deformations [31]. These two different membrane deformation mechanisms are indicated schematically in Fig. 8.

A natural mechanical question we might imagine starting with is the energetic cost associated with bending the membrane. The free energy cost to deform a tiny patch of membrane is codified in the form of the so-called Helfrich-Canham-Evans free energy [11]. For a tiny patch of membrane with area ΔA_{patch}, the free energy cost to bend it is given by

$$\text{energy to bend a membrane patch} = \frac{\kappa_B}{2}\left(\frac{1}{R_1}+\frac{1}{R_2}\right)^2 \Delta A_{\text{patch}}, \tag{3}$$

where κ_B is the membrane bending rigidity and R_1 and R_2 are the principal radii of curvature of the patch of membrane. Note that the membrane bending rigidity has units of energy since the unit of the factor in parentheses is $1/\text{area}$ which is cancelled by ΔA_{patch} which has units of area. The values of R_1 and R_2 characterize the curvature of the surface at the point of interest. Specifically, if we visit a particular point on the surface, we can capture the curvature by using two orthogonal circles whose radii are chosen so that those two circles most closely follow the shape of the surface at that point. Given the free energy in Eq. (3), we can find the total free energy of a given deformed membrane configuration by adding up the contribution from each little patch as

$$E_{\text{bend}} = \frac{\kappa_B}{2}\int dA \left(\frac{1}{R_1(x,y)}+\frac{1}{R_2(x,y)}\right)^2, \tag{4}$$

where now we acknowledge that the curvature (as measured by R_1 and R_2) is potentially different at each point on the surface. Of course, the scale of this energy is dictated by the bending rigidity κ_B. Our discussion has neglected a second topological contribution to the membrane deformation energy related to the

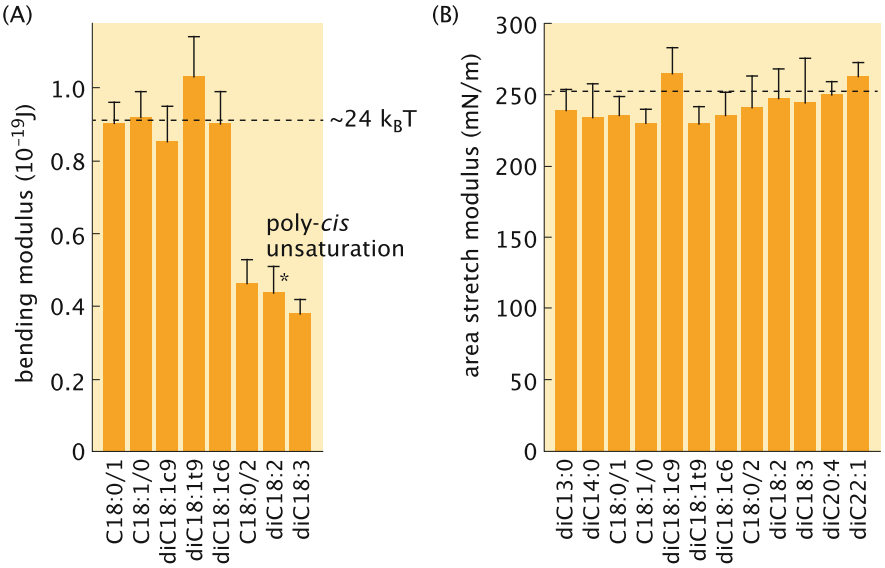

Fig. 9 Elastic moduli characterizing membrane bending and stretching. (**a**) Values for the membrane bending rigidity. Each value corresponds to a different lipid with the values showing a range of tail lengths and tail saturation. (**b**) Values for the area stretch modulus. All values obtained using pipette aspiration experiments [32]

Gaussian curvature, though clearly such terms will be of interest in the context of the topologically rich membrane structures found in cell organelles [11].

A wide range of experiments on a variety of different lipids suggest the rule of thumb that the bending modulus (κ_B) for lipid bilayers is in the range 10–25 k_BT [32, 33]. Characteristic values of the membrane bending rigidity for phospholipid bilayers are shown in Fig. 9a. We will freely use k_BT for our energy units and note the conversion factors $k_BT \approx 4.1$ pN nm $\approx 4.1 \times 10^{-21}$ J. The presence of sterols in lipid bilayers can increase those numbers to $\approx 100\, k_BT$ [34]. Interestingly, even measurements on biological membranes derived from the ER and Golgi apparatus report a membrane rigidity of $\kappa_B \approx 3 \times 10^{-19}$ J $\approx 75\, k_BT$ (BNID 110851), only a factor of three larger than the values for phospholipid bilayers reported in Fig. 9a [35, 36].

Another important question we can ask about membrane deformations is the energy cost for changing the area of the membrane as seen in Fig. 8. When we stretch a membrane away from its equilibrium area, a consequence is the development of a tension in that membrane. One way to understand the magnitude of membrane tensions is by appealing to a so-called constitutive equation which loosely speaking relates force and membrane geometry. In particular, the mechanics of membrane stretching is often described by the constitutive equation

$$\tau = K_A \frac{\Delta A}{A_0}, \tag{5}$$

where K_A is the area stretch modulus and ΔA is the area change. To figure out the tension, we compute the change in area, normalize by the total unstressed area A_0, and then multiply by the modulus K_A. In general, when we change the area of a patch of membrane by some amount ΔA, the corresponding free energy cost can be written as

$$\text{stretching energy} = \frac{K_A}{2}\left(\frac{\Delta A}{A_0}\right)^2 A_{\text{patch}}, \tag{6}$$

where note that the units of the area stretch modulus K_A are energy/area. Several examples of the values adopted by the area stretch modulus are shown in Fig. 9b, which gives the interesting insight that for a range of tail lengths and degrees of saturation, the area stretch modulus is nearly constant.

The actual magnitudes of the tensions in the membranes of both vesicles and cells can vary over a wide range and even the underlying mechanistic origins of these tensions are different depending upon what regime of tension we are considering. Interestingly, the energetics of area change is a subtle one in the same way as the energetics of stretching a polymer like DNA is. Specifically, let's remind ourselves of the subtleties associated with DNA stretching as a prelude to thinking about membrane stretching [4, 11]. In the "force free" state, DNA will be folded up and compact since such states have lower free energy in part because the entropy of the compact conformation is higher. To stretch DNA, the free energy cost can be thought of as being almost entirely entropic, meaning that with increasing stretch, there are fewer and fewer configurations available to the DNA and hence the entropy *decreases*, resulting in a net increase in free energy. It is only when the DNA is stretched to its full contour length that we enter a different regime that actually involves molecular bond stretching. Because the mechanisms in these regimes are different, it should not surprise us that they are actually characterized by different mechanical stiffnesses. Similar intuition emerges for the membrane case.

By analogy with polymer stretching, we can think of the energetic cost associated with membrane deformations in much the same way. That is, for a floppy (low tension) membrane, stretching the membrane has an associated free energy cost that results from "pulling out the wrinkles," and is effectively entropic [11]. At higher tensions, the actual bond stretching effect intervenes. Though very few systematic insights have been obtained for thinking about the membranes within cells, a series of rigorous, systematic studies in lipid bilayers have set the standard in the field [32]. At even higher tensions, lipid bilayer membranes will actually rupture with the rupture tensions occurring between 5 and 10 mN/m depending upon the type of lipids in question [37].

Though there are fewer systematic measurements for cellular membranes, some clever experiments have shed light on this topic as well. The tension measured in ER membrane networks has a value of 1.3×10^{-2} mN/m while that measured in the Golgi membrane is given by 0.5×10^{-2} mN/m [38]. These numbers are quite small as can be seen by comparing them to the membrane rupture tension which is a thousand times larger with a range of 5–10 mN/m as noted above [37]. Note

also that the subject of membrane tension is a tricky one in the cellular setting because measured tensions have many contributions including from the underlying cytoskeleton and the battery of molecular motors associated with it [39]. There is an excellent review featuring both a clear discussion of the different methods and the range of measured tensions [40]. Table 1 of that review includes an exhaustive listing of measured membrane tensions as well as the caveats associated with each such measurement.

5 The Dynamic Membrane

Perhaps the defining feature of biological membranes is that they serve as barriers between some compartment of interest (the cytoplasm, the Golgi apparatus, the nucleus, the endoplasmic reticulum, etc.) and the rest of the world. The very word "barrier" points toward underlying molecular rules that determine the rate at which molecules cross through or move within membranes, and thereby regulate how a cell distinguishes itself from the environment. In this section, we begin by exploring the permeability of biological membranes to various molecular species. After that, we then turn to the diffusive properties of molecules within the membrane.

One of the key ways we characterize membrane permeability is to ask the question of how many molecules cross a given area of membrane each second, a quantity defined as the flux, j. In particular if we have a difference in concentration of some species across the membrane given by Δc, then in the simplest model the flux is given by

$$j = -p\Delta c, \tag{7}$$

where the parameter p is the permeability of interest here. Note that a more rigorous treatment of the flux invokes the chemical potential difference across the membrane, though for our purposes this simple linearization suffices [41, 42]. The units of the permeability can be deduced by noting first that the units of j are

$$\text{units of } j = \frac{\text{number of molecules}}{L^2 T}. \tag{8}$$

Here we adopt the standard strategy when examining units of physical quantities of using the symbol L to signify units of length and T to signify the units of time [43]. Given these conventions, the units of concentration are

$$\text{units of } c = \frac{\text{number of molecules}}{L^3}. \tag{9}$$

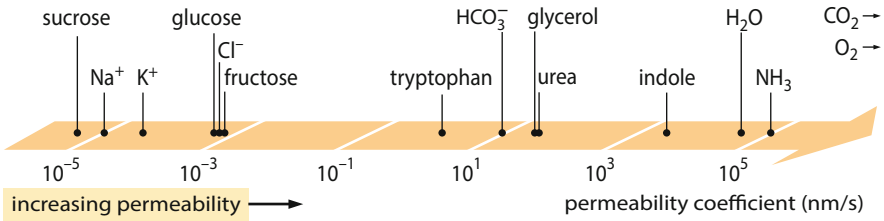

Fig. 10 Range of membrane permeabilities. Permeability coefficients for a number of different lipid species showing the huge dynamic range in permeability

The requirement that the units on the two sides of the equation balance implies that the units of the permeability itself are

$$\text{units of } p = \frac{\frac{\text{number of molecules}}{L^2 T}}{\frac{\text{number of molecules}}{L^3}} = \frac{L}{T}. \tag{10}$$

In the remainder of the paper, we will report units of permeability in nm/s, though often one finds values reported in cm/s as well.

The first and probably most important thing we should say about the numerical values adopted by membrane permeability is that there is no such thing as *the* membrane permeability. That is, the rate at which molecules pass across membranes is an extremely sensitive function of which molecules we are discussing as well as the type of molecules making up the membrane itself [10, 37, 44]. Figure 10 makes this point clear by reporting the range of values for permeability for a number of different molecular species revealing a more than 10-order-of-magnitude range of permeabilities, with the membrane being effectively impermeable to ions such as Na^+ and K^+, while for water molecules, the permeability is ten orders of magnitude larger. Though this doesn't rival the 30 order-of-magnitude range that is found for electrical conductivities of different materials, these numbers still imply a huge difference in the transport properties of different molecules across membranes.

How are such permeabilities measured? One approach to measuring these membrane permeabilities is the use of radioactive tracer molecules. By setting up a membrane separating two aqueous regions with different compositions, one can measure the accumulation of the tracer in one region as a result of flux from the other region over time [44]. A second important set of measurements for water permeability were performed using giant unilamellar vesicles using the so-called micropipette aspiration method where an osmotic pressure is applied across the membrane and the resulting flux of water across the membrane is measured. Here the idea is that a pipette with a characteristic diameter of several microns is used to grab onto a vesicle with a diameter of roughly 10 µm or larger. By applying a suction pressure, the tension of the vesicle can be monitored. Further, by using video microscopy, the volume of the vesicle can be carefully monitored, giving a sense of

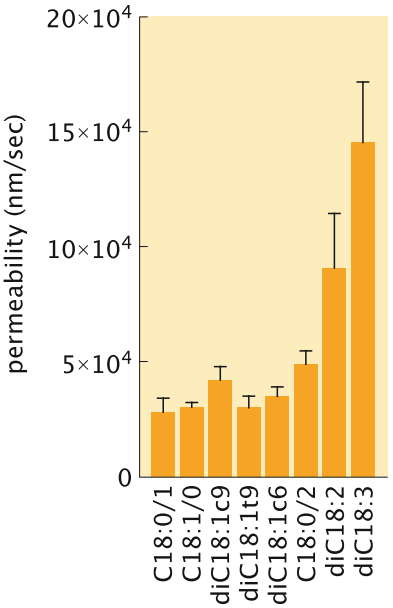

Fig. 11 Range of membrane permeabilities for water. Measurements made at 21 °C using the micropipette aspiration technique in conjunction with video microscopy to monitor vesicle size [37]

the rate at which the vesicle is inflated as a result of mass transport of water across the membrane. The results of such measurements for a set of different lipid types are shown in Fig. 11, with values entirely consistent with those shown schematically in Fig. 10.

The classic work of Hodgkin and Huxley offered many important insights. To my mind, one of the most interesting arguments that they made is a testament to the role of clear theoretical (and quantitative) thinking in biology. In particular, they argued that the membrane permeability to ions such as Na^+ and K^+ must change transiently and substantially to permit key ions across the otherwise impermeable membrane (see Fig. 10 to get a sense of the extremely low permeability of charged ions). Specifically, they introduced a highly nonlinear permeability response that suggested that there must be molecules in the membrane of the cell that could selectively change the permeability in response to changes in driving forces such as the membrane potential, effectively hypothesizing the existence of ion channels before they were known.

We now know that biological membranes are littered with batteries of different channels and pumps whose job it is to transiently alter the permeability of the membrane or to actively transport molecular species across it. These membrane proteins are responsible for many physiologically important functions including the transport of ions and sugars such as glucose and lactose that are critical to the cellular economy. Ions typically pass across ion channels at rates between 10^7 and 10^9 ions per second, though of course this rate depends upon the concentration difference across the membrane itself (BNID 103163,103164). Glucose transporters have a much lower characteristic rate of several hundred sugars per second (BNID

102931, 103160) while bacterial lactose transporters have a characteristic rate of 20–50 sugars per second (BNID 103159). Though here we report on the rates associated with several well-known membrane proteins, more generally, the rates at which the various membrane proteins that are responsible for transport operate are not that well known, with a dearth of modern data spanning the range of different membrane transporters (BNID 103160) [45].

A second kind of membrane dynamics different from the transport *across* the membrane described above is diffusion of molecules laterally within the membrane. As already noted throughout the chapter, the membrane is a highly heterogeneous composite of lipids and proteins and when thinking about the diffusive dynamics within the membrane, we need to do so on a molecule-by-molecule basis. Since we are thinking about membranes, the first class of molecules we might be interested in characterizing are the lipids themselves [46–50]. For example, in eukaryotic cell membranes, by using the clever method of fluorescence-recovery-after-photobleaching (FRAP), a lipid diffusion constant of 0.9 $\mu m^2/s$ was measured [46]. This diffusion constant is roughly tenfold lower than the values that would be found in a model lipid bilayer membrane [51]. More recent measurements confirm these classic numbers (see Figure 4 of Ref. [50], for example).

It is of great interest to characterize the in-plane diffusion not only of the lipids themselves, but also of the proteins that populate those membranes. Figure 12 gives examples of membrane diffusion constants for several different membrane

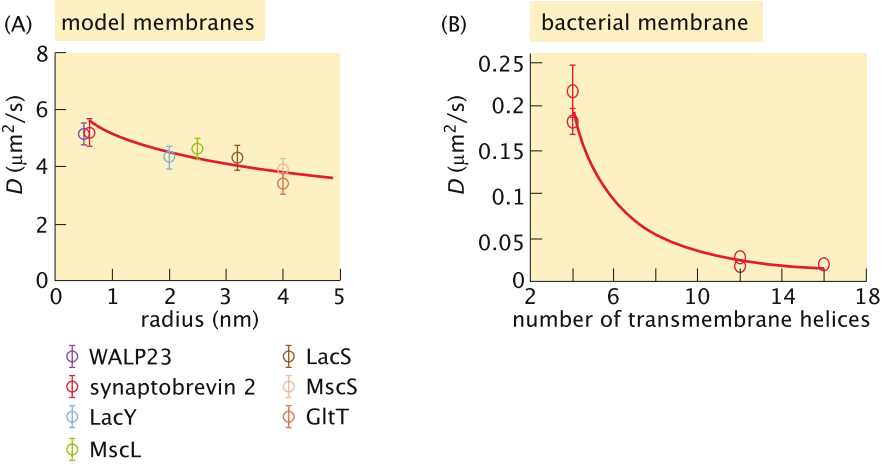

Fig. 12 Range of diffusion coefficients. (**a**) Diffusion coefficients for different membrane proteins measured using fluorescence correlation spectroscopy in giant unilamellar vesicles showing dependence on protein size. The red line is a fit using the Saffman-Delbrück model which characterizes membrane diffusion as a function of the size of the diffusing molecule [52, 53]. (**b**) Diffusion coefficients for different membrane proteins measured using fluorescence recovery after photobleaching (FRAP) in the *E. coli* cell membrane. The red line is an empirical fit as a function of the number of transmembrane helices in the protein. The names refer to particular membrane proteins used in the experiments. (**a**) adapted from [54] and (**b**) adapted from [55]

proteins. Further, we need to acknowledge the large differences in lateral diffusion coefficients between model membranes such as are found in giant unilamellar vesicles where the values of diffusion coefficients for membrane proteins are 1–10 $\mu m^2/s$ [54] and those in native membranes where membrane proteins are characterized by diffusion coefficients that are several of orders of magnitude lower with values of 0.01–0.1 $\mu m^2/s$ [50, 55–57]. However, these measurements are more nuanced than first meets the eye and the results for several membrane proteins have been shown to depend upon the timescales over which the diffusion is characterized [56]. In particular, using the FCS method which probes diffusion on short length and timescales, both the TAR receptor and TetA (a tetracycline antiporter) were found to have diffusion constants of 4.2 and 9.1 $\mu m^2/s$, respectively, to be contrasted with the values of 0.017 and 0.086 $\mu m^2/s$, respectively, found when using the FRAP measurement. Indeed, as we will note in the final section of the chapter, the question of how best to move from biological numeracy in model membranes to biological membranes with their full complexity is one of the key challenges of the coming years of membrane research.

6 The Electrical Membrane

A membrane has many different properties as shown in Fig. 1. So far, our picture of membranes has focused on their mechanical and transport properties. However, our discussion of action potentials and the pathbreaking work of Hodgkin and Huxley already hinted at the view that membranes can also be thought of as circuit elements. Specifically, part of this chapter's very business is to illustrate some of the different *abstract* ways of describing membranes and what *effective* parameters to attribute to them. We now jettison the view of a membrane as a mechanical object, instead focusing on it as a collection of resistors and capacitors as shown in one of the panels of Fig. 1.

The picture already developed under the heading of the "Electrical Membrane" in Fig. 1 tells us that in the presence of an electric potential, a lipid bilayer behaves as an array of resistors and capacitors in parallel. One way to measure the electrical conductance across a membrane patch is to form a lipid bilayer membrane across a hole separating two solutions. Then, different voltages are applied across the membrane and the current–voltage characteristics are measured, with the membrane conductance then determined by using the slope of these current–voltage curves. In our discussion of the electrical membrane we characterize electrical properties on a per unit area of membrane basis. For the conductance, a series of measurements like those described above for a number of different charged species result in a range of values for the bare membrane conductance of roughly 1–5 nS/cm^2 [58, 59]. To get a sense of how small the membrane conductance is, note that if we consider a characteristic conductance of 1 nS for an ion channel such as the mechanosensitive channels found in bacteria [60], if we normalize by the area this means that the

channel conductance is more than ten orders of magnitude larger than that of the membrane itself.

But membranes have more electrical properties than their conductance alone [4]. Capacitance is a measure of the ability of a circuit element to store charge. A local disruption of charge neutrality is permitted near surfaces. In particular, in this setting, the capacitance is defined as the ratio of the excess charge on either side of the membrane and the membrane potential, $C = q/V_{mem}$. The capacitance of a patch of the cell membrane can be approximated by thinking of it as a parallel plate capacitor. The charge on the capacitor plates is $\pm\sigma A_{\text{patch}}$, where σ is the excess charge per unit area of membrane, and A_{patch} is the area. The electric field inside a parallel plate capacitor is uniform and equal to $\sigma/(\varepsilon_0 D)$, where D is the dielectric constant of the material between the plates. Therefore the potential drop across the membrane is $V_{mem} = \sigma d/\varepsilon_0 D$, where d is the thickness of the membrane, or the distance between the plates of the parallel plate capacitor. Dividing the charge by the membrane voltage leads to the formula, $C = \varepsilon_0 D A_{\text{patch}}/d$, for the capacitance of a patch of membrane. Since the cell membrane has a thickness of $d \approx 5\,\text{nm}$ and a dielectric constant $D_{mem} = 2$, its capacitance is predicted to be $C_{\text{area}} = C/A_{\text{patch}} \approx 0.4\,\mu\text{F/cm}^2$. The typical measured value for the capacitance per unit area in cell membranes is $C_{\text{area}} = 1\,\mu\text{F/cm}^2$ [61–63].

We have already discussed the century long quest to understand the size of lipid molecules and the membranes they make up. We learned that one branch of these investigations passed through the enormously impressive work of Pockels, Rayleigh, and Langmuir. Amazingly, a completely independent line of enquiry in the hands of Fricke related to the electrical properties of membranes led to nearly the same result [61]. Using these ideas, we can recast the measured value of the membrane capacitance as a result for the membrane thickness as

$$d = \frac{\epsilon}{(C/A)} = \frac{2\epsilon_0}{(C/A)} \approx \frac{2 \times 8.8 \times 10^{-12}\,\text{F/m}}{0.4 \times 10^{-2}\,\text{F/m}^2} \approx 4\,\text{nm}, \tag{11}$$

a beautiful result astonishingly close to the value obtained using the equation of state of monolayers by Pockels, Rayleigh, and Langmuir. Note that to obtain this result, we rewrote the conventional membrane capacitance of $0.4\,\mu\text{F/cm}^2$ in the more appropriate SI units as $0.4 \times 10^{-2}\,\text{F/m}^2$. Further, whereas Frick used a relative dielectric constant of 3, the estimate used here is based upon the value of 2. In light of the measurement of the membrane capacitance, scientists such as Fricke realized that this would provide yet another sanity check on the membrane thickness [61]. In this era where many scientists seem almost to have scorn for the idea of figuring things out without seeing them directly, the determination of the thickness of lipid bilayers long before the advent of direct techniques such as electron microscopy should give readers pause before casually dismissing results that come from indirect measurements.

7 The Fermi Membrane: Thinking Up Membranes

So far, this chapter has been an ode to biological numeracy in the context of membranes, showing us the many different ways in which we can quantitatively describe our hard-earned understanding of these fascinating structures. These numbers are summarized in Table 2. But in the abstract, such numbers are often boring and sometimes useless, or worse yet, misleading. To my mind, numbers that characterize the world around us are only really interesting when put in the context of some argument or reflection. For example, we know that if we drop an object near the surface of the Earth, in the first second, it will fall roughly 5 m. So what? In the powerful hands of Newton, this innocuous number became part of his inference of the law of universal gravitation. There is a direct intellectual line from a knowledge of the radius of the Earth and the distance to the moon to Newton's estimate leading him to further trust the idea that the force of gravity falls off as the square of the distance. In that case, he realized that the distance to the moon is roughly 60 times larger than the radius of the Earth, meaning that the acceleration of the moon as it "falls" toward the center of the Earth should be $(60)^2 = 3600$ times smaller than that associated with that apocryphal apple falling from Newton's tree. To finish off his estimate, he asked the question of how far the moon falls compared to how far the apple falls when watched for the same time and found them to "answer pretty nearly," with the moon falling roughly 1/3600 as much in 1 s as the 5 m a falling

Table 2 Membranes by the numbers

Membrane parameter	Range of parameter values	BNID
Lipid length	≈2.5–3.5 nm	See Table 1
Lipid area	≈1/4–3/4 nm^2	See Table 1
Number of lipids per cell (bacterium)	$\approx 2 \times 10^7$	100071
Bending rigidity	10–25 $k_B T$	105297
Area stretch modulus	200–250 mN/m (or $\approx 50\, k_B T/\text{nm}^2$)	112590, 112659
Membrane tension	$10^{-4} - 1\, k_B T/\text{nm}^2$	110849,112509, 112519
Rupture tension	1–2 $k_B T/\text{nm}^2$	112489, 110911
Membrane permeability (water)	10–50 μm/s	112488
Membrane capacitance	≈1 $\mu\text{F/cm}^2$	110759, 109244, 110802
Membrane resistance	$0.1\text{–}1.5 \times 10^9\ \Omega\,\text{cm}^2$	110802
Membrane potential	100 mV	109775, 107759
Diffusion constant (lipid)	≈1 $\mu\text{m}^2/\text{s}$	112471, 112472
Diffusion constant (membrane protein)	≈0.02–0.2 $\mu\text{m}^2/\text{s}$	107986

A summary of the key numbers about membranes discussed throughout the chapter for easy reference. Numbers reported are "typical" values and should be used as a rule of thumb. For a more detailed description of parameter values, the reader should use the Bionumbers database through the relevant BNID. Also see Box 1 of [14]

body at the surface of the Earth falls in that same time interval. But what does this have to do with our quantitative musings on membranes? To my mind, it illustrates how powerful simple numerical arguments can sometimes be to help us see whether our way of thinking is consonant with the known facts about a system.

Inspired by the long tradition of simple estimates when faced with numerical magnitudes to describe the world around us, we now examine the ways in which the numbers presented throughout the chapter can help us to better understand membranes and the biological processes that take place at them. Indeed, we are inspired by the notion of the so-called Fermi problems introduced at the beginning of the chapter where the goal is to try to develop simple numerical estimates for various quantities of interest by pure thought. Not only does the Fermi approach allow us to estimate key magnitudes, but even more importantly, it is one of the most powerful ways I know to make sure that the stories we tell about our data actually make sense. In this section, we ask ourselves whether we can understand some of the numerical values reported throughout this chapter as well as what key scaling results we should bear in mind when thinking about membranes. We pass through each of the sections of the chapter in turn, each time taking the opportunity to reflect on the numbers we have seen.

Size and Shape Redux In the first part of the chapter, we considered different ways of characterizing the size and shapes of membranes and the molecules that make them up. This led us to the fascinating experiments of Langmuir that used the relationship between tension and area as a way of determining the size and shape of lipids. Here, our aim is to use order-of-magnitude thinking to try and put those numbers in perspective. As an example from everyday life where a simple numerical estimate of the Fermi type can help us build intuition by giving us a sense of the relative sizes of membranes and the cells they envelop, we consider the fuselage of an airplane. One of the most popular tourist destinations in Seattle is the factory of Boeing where one can see giant airplanes such as the 747, 777 and 787 in the process of assembly. As part of that tour one is treated to the view of a cross-section of a 747 fuselage which gives a sense of just how thin the skin of an airplane really is. For the perceptive flyer, this same observation can be made upon entering the plane by looking at the fuselage near the door. What one notices is that the exterior shell of the plane is less than a centimeter thick while the overall diameter of that very same fuselage is roughly 5 m, resulting in an aspect ratio of 1:500. Interestingly, the aspect ratio of cell membrane width to cell size is quite comparable to those of an airplane fuselage. For a 2 micron cell size, typical of a bacterium, the 4 nm thickness of its cell membrane implies a similar aspect ratio of 1:500.

Concentrations The section on concentrations reminded us that cell membranes are made up of molecules and that even in tiny bacterial cells, there are tens of millions of such molecules of hundreds of different types. A very simple order-of-magnitude result that emerges from these numbers is a naive estimate of the rates of lipid synthesis. Specifically, if the membrane area has to double during the cell cycle, this tells us that the number of lipids in the cell membrane has to double. For a bacterium such as *E. coli*, this means that if a typical bacterium has 2×10^7 lipids

and the cell cycle is roughly 2000 s, then the rate of lipid synthesis is roughly

$$\text{bacterial lipid synthesis rate} = \frac{\text{number of lipids}}{\text{cell cycle time}} \approx \frac{2 \times 10^7 \text{ lipids}}{2 \times 10^3 \text{ s}} \approx 10^4 \text{ lipids/s}. \tag{12}$$

It is deeply interesting to think of how the many different types of lipids are each synthesized with the correct rates to maintain the overall concentration distribution.

Another critical concern in our discussion of the chemistry of membranes was how to think about the relative abundance of lipids and proteins. One of the interesting ways to broach this question is through reference to the fraction of genomes that is devoted to membrane proteins. We can examine this question both from a genomic point of view and from a proteomic point of view. Scientists have become increasingly adept at reading genomes and as a result, by recognizing features such as transmembrane alpha helices, it is possible to estimate the fraction of proteins that are membrane proteins with a rule of thumb being that roughly 1/4 of the protein coding genes correspond to membrane proteins [64]. From a proteomic point of view, this question can be addressed by asking what are the copy numbers of these different membrane proteins. Given that a bacterium such as *E. coli* has several million proteins in total, what fraction of those proteins are in the membrane? To give a feeling for the answer to that question, we ask about the copy numbers of some key membrane proteins. Specifically, we consider membrane transporters, components of the ATP synthesis machinery, and the receptors of chemotaxis to give an idea of the molecular census for some of the most important classes of membrane proteins. Transport of sugars across the cell membrane is one of the most critical activities of growing bacteria. Recent ribosome profiling measurements and mass spectrometry measurements tell us that the number of copies of sugar transporters for glucose (ptsI proteins, a component of the phosphoenolpyruvate-dependent sugar phosphotransferase system) has a copy number of between roughly 3000 copies per cell and 15,000 copies per cell depending upon the growth conditions [65, 66]. We examine the relevance of these numbers in the context of membrane dynamics below. ATP synthase is one of the most important of membrane protein components in almost all cell types. In *E. coli* the ATP synthase complex is built up of many different subunits. For those subunits that come with a stoichiometry of one molecule per complex, their copy number ranges between 3000 and 10,000 copies per cell [65, 66]. Knowing these numbers provides a powerful sanity check on the rate of ATP production per cell since with roughly 3000 such synthases, each rotating at about 300 turns per second (BNID 104890), this means that over a cell cycle of 2000 s, on the order of 10^9 ATPs will be generated, comparable to the number needed to run the cellular economy [4, 19]. Finally, for the chemotaxis receptors such as Tar and Tsr, the copy numbers can be as low as several thousand and as high as nearly 40,000 per cell (BNID 100182) [67, 68]. These numbers give us a sense that if roughly 1000 of the 4000 or so *E. coli* proteins are membrane proteins and each comes with a copy number of roughly 1000, then a first simple

estimate is that there are a total of 10^6 membrane proteins distributed across the inner and outer membranes of these cells.

Membrane Mechanics Our section on membrane mechanics gave us a basis for thinking about many key processes that take place in cell biology. One such example that begins to shed light on the free energy demands associated with sculpting membranes into different shapes is that of membrane vesicles. From the standpoint of the energetic description given in Eq. (4), we can make a simple estimate of the free energy cost required to create spherical vesicles such as those found at synapses. Since for a sphere the two radii of curvature are equal and have a value R and the total area of each such sphere is $4\pi R^2$, Eq. (3) instructs us to sum up

$$E_{\text{vesicle}} = \frac{\kappa_B}{2}\left(\frac{1}{R} + \frac{1}{R}\right)^2 A_{\text{sphere}} = \frac{\kappa_B}{2}\frac{4}{R^2}4\pi R^2. \tag{13}$$

This implies the fascinating and for many people, counterintuitive result, that the energetic cost for vesicle formation due to membrane bending is $E_{\text{vesicle}} = 8\pi\kappa_B \approx 250\text{–}500\, k_{\text{B}}T$, completely independent of the size of the vesicle.

A second example from membrane mechanics is to try to estimate the strain suffered by a membrane at the time of rupture. To estimate this magnitude, we can use

$$\tau_{rupture} = K_A \frac{\Delta A_{rupture}}{A}, \tag{14}$$

where the subscript *rupture* indicates the value of the parameter at rupture. If we use the values provided in Table 2, we can estimate the rupture strain as

$$\frac{\Delta A_{rupture}}{A} = \frac{\tau_{rupture}}{K_A} \approx \frac{5\,\text{mN/m}}{200\,\text{mN/m}} \approx 2.5\%. \tag{15}$$

Often people are surprised by how small the rupture strains really are since we have an impression that lipid bilayers are floppy, squishy, and highly deformable materials.

Membrane Dynamics In the section on the dynamic membrane, we considered the permeability of membranes to various molecular species. One simple estimate that we can do to get a sense of the meaning of the permeability is to ask how many molecules cross the cell membrane each second given some concentration difference. Given the concept provided in Eq. (7), we can estimate

$$\frac{dN}{dt} = j \times A, \tag{16}$$

Given a typical membrane permeability for water of order $p \approx 100\,\mu\text{m/s}$ and considering a typical concentration difference of salt across the cell membrane when

cells are subjected to an osmotic shock of order 100 mM $\approx 10^8$ molecules/μm^3, [69] for example, we can make the simple estimate that

$$j \times A = p\Delta cA \approx 100\,\mu m/s \times 10^8/\mu m^3 \times 5\,\mu m^2 \approx 5 \times 10^{10}\,s^{-1}. \tag{17}$$

These numbers are interesting to contrast with the rate of transport of molecules across ion channels. Specifically, given the conductivity of a channel such as the mechanosensitive channel of large conductance (MscL), we find that the opening of a single channel yields a flow rate of several molecules per nanosecond, quite comparable to the flow rate of water across the membrane itself [60, 70].

One of the most interesting estimates concerning membrane dynamics that we can consider focuses on the mass and energy economy of a cell. To this day, I still marvel at the fact that one can take 5 mL of liquid containing some salts and sugars, inoculate that solution with a single bacterium, and 12 h later one will find as many as 10^9 cells per mL of solution. Effectively, what has happened is that the molecules in the medium have been taken up by that bacterium, used to construct building materials and energetic molecules such as ATP and then used them to construct a new cell. This process repeats over and over again every 20 or so minutes. These observations raise an obvious Fermi question: is the rate of membrane transport of sugar molecules, for example, fast enough to keep up with the needs of the cell to reproduce [19]. To approach that question, we consider the flux of sugar across the membrane using the numbers presented above, namely that there are 3000–15,000 sugar transporters per cell, each of which is able to take up sugars at a rate of several hundred sugars/sec (BNID 102931, 103160, 100736). We can get a feeling for the number of sugars taken up per cell cycle as

$$\begin{aligned}\text{flux of sugar} &= (10^4 \text{ transporters}) \times (300 \text{ sugars/transporter sec}) \times (2 \times 10^3 \text{ s}) \\ &\approx 6 \times 10^9 \text{ sugars}.\end{aligned} \tag{18}$$

This number is of the right order, though probably on the low side of what is needed to power the cellular economy and raises interesting questions about possible rate-limiting steps in cellular growth [4, 19].

Just as we did in the section of the chapter on the dynamic membrane, it is of interest to focus not only on the dynamics across the membrane, but also on the dynamics of molecules within the membrane. Specifically, one question of interest is how long does it take molecules to travel across the cell membrane given the measured diffusion constants? To answer this question, we appeal to the simple estimate that the timescale for diffusing a distance L is given by

$$t_{\text{diffusion}} \approx \frac{L^2}{D}. \tag{19}$$

For a bacterial cell with dimensions of several microns, this means that the diffusion time to explore the membrane is

$$t_{\text{diffusion}} \approx \frac{1\,\mu\text{m}^2}{1\,\mu\text{m}^2/\text{s}} \approx 1\,\text{s}, \tag{20}$$

where we have taken a diffusion coefficient for a lipid of $1\,\mu\text{m}^2/\text{s}$. This characteristic timescale is confirmed in fluorescence-recovery-after-photobleaching (FRAP) experiments (see [55], for example).

The Electrical Membrane The electric fields across biological membranes are surprisingly high as can be estimated by using

$$E \approx \frac{V}{d} \approx \frac{100\,\text{mV}}{4\,\text{nm}} \approx \frac{100 \times 10^{-3}\,\text{V}}{4 \times 10^{-9}\,\text{m}} \approx 2.5 \times 10^7\,\frac{\text{V}}{\text{m}}. \tag{21}$$

Note that this field is an order of magnitude higher than the electric fields associated with dielectric breakdown in the atmosphere. And yet, fields five times as high have been measured in membranes with no evidence for any anomalous behavior [71].

This section had as its ambition to give a sense of how the numbers summarized in Table 2 can be used to develop intuition [3, 4]. In fact, more than anything, this brief section is an invitation to others to look for meaning in the hard won outcome of the recent work to extend membrane numeracy.

8 The Missing Membrane Numbers

As a final send-off of this brief ode to biological numeracy for membranes, we reflect on the state of our art and how it can be improved. Despite a long list of truly amazing successes, there are still many things not to like about the current status of biological numeracy, not only in terms of how well we actually know the numbers, but also in terms of what those numbers might mean for a deeper understanding of biological systems. The goal in this final section is to make an attempt at critiquing both this article and the current state of the art with the aim of suggesting future directions. Though the "by the numbers" approach has become something of a cliche, my opinion remains that there is much to be gained by pushing hard with this approach on each of the many diverse and wonderful facets of biology [19, 72–77].

One of the first weaknesses of biological numeracy in the membrane setting (and beyond) is the need to establish measurements of sufficient precision that we can confidently report on measured values. For example, there is already much evidence that biological membranes "care" about their lipid composition. It would be a powerful addition to our ability to ferret out molecular mechanisms to be able to examine these membrane compositions for all organelles as a function of time

and for a variety of different environmental conditions. First steps in this direction have been made in thinking about proteomes with one of my favorites reporting on the proteome of *E. coli* in more than 20 distinct conditions [66]. Absent accurate and reproducible measurements in the membrane setting, we are handcuffed in our efforts to construct a fruitful dialogue between theory and experiment [78, 79].

A second important challenge for the future of membrane numeracy is the vast differences between model membranes and the real world of plasma and organellar membranes. Effectively each and every section of this chapter—size and shape, composition, mechanics, transport, electrical properties—is bereft of any deep understanding of how all of the heterogeneities of real membranes might alter the numbers, and what the significances of such alterations might be. The advent of mass spectrometry in conjunction with ever more sophisticated microscopies as a window onto membrane composition has left in their wake a host of mysteries and challenges. As highlighted in Figs. 6 and 7, and indicated widely in other literature,[18, 20–28] cells care about their lipid composition. What is lacking is a conceptual framework that tells us what these numbers really mean in terms of biological function, what they imply about the regulation of lipid biochemistry and perhaps most importantly, what they imply about the evolution of life.

Another example that strikes me as an exciting challenge to our current thinking broadly concerns the question of cellular shape, and the shapes of organelles, more specifically. The images shown in Fig. 4 make clear the great diversity of membrane shapes. The study of mitochondria as a concrete example presents challenges at every turn [15]. My personal favorite remains the intriguing membrane structures found in the outer segments of photoreceptors (see Fig. 4b). In the context of the ideas presented in this chapter, one of the ways that people have attacked questions of shape traditionally has been through the approach of free energy minimization [11, 80]. But there are interesting, novel alternatives that are now in play. One approach focuses on the role of dynamics where there is an interplay between differential growth and the cost of elastic deformations as characterized by the kinds of mechanical parameters reported here [81, 82].

Thus far our discussion has largely focused on the physical properties of membranes. But there is another interesting angle on membranes that is more related to their evolutionary significance. Interestingly, one of the simplest acts of biological numeracy, namely counting, can provide evolutionary insights. Specifically, the number of membranes surrounding an organelle is perhaps the best indicator of its evolutionary origins, with the argument being made that more than one such membrane means that organelle has an endosymbiotic origin and more than two such membranes might imply nested symbioses [83–85].

We are in the midst of a biological revolution. The pace of discovery in the study of living matter is dizzying in all corners of biology. The central thesis of this article is enlightenment through biological numeracy. That is, as part of our attempt to make sense of the living world, we can sharpen our questions and be more rigorous in our demands about what it means to really understand something [78, 79]. One of the ways of placing those demands is to ask for an interplay between our experimental data and our theoretical understanding of biological processes. The

study of biological membranes is one of the most important areas for future work and in many ways has not kept pace with insights into genomes and the proteins they code for because of a want of appropriate tools. It is hoped that the chapters in this book will serve as an inspiration for the development of the tools that will make membrane numeracy as sophisticated as is our understanding of nucleic acids and proteins.

Acknowledgements One of the best parts of being a member of the scientific enterprise is all the smart and interesting people we get to interact with. In preparing this chapter I sent out a survey to many experts in membrane biology and biophysics and was overwhelmed with the thoughtful responses that I received from many colleagues. I am grateful to Olaf Andersen, Patricia Bassereau, Joel Dacks, Markus Deserno, Evan Evans, Ben Freund, Jay Groves, Christoph Haselwandter, Liz Haswell, KC Huang, Ron Kaback, Heun Jin Lee, Mike Lynch, Bill Klug, Jane Kondev, Ron Milo, Uri Moran, John Nagle, Phil Nelson, Bert Poolman, Tom Powers, Doug Rees, James Saenz, Pierre Sens, Victor Sourjik, Stephanie Tristram-Nagle, and Tristan Ursell for useful discussions. I am especially grateful to Olaf Andersen, Markus Deserno, Christoph Haselwandter, James Saenz, Pierre Sens, and Tristan Ursell who have been patient and persistent in advancing my membrane education, though obviously all shortcomings in this chapter are due to my failure to absorb that education and are no fault of their own. I am privileged to be entrusted by the National Science Foundation, the National Institutes of Health, The California Institute of Technology and La Fondation Pierre Gilles de Gennes with the funds that make the kind of work described here possible. Specifically I am grateful to the NIH for support through award numbers DP1 OD000217 (Director's Pioneer Award), R01 GM085286, and 1R35 GM118043-01 (MIRA). I am also grateful to the Kavli Institute for Theoretical Physics where much of this chapter was written. More generally, this article is part of an adventure that I have undertaken with Ron Milo and Nigel Orme (our illustrator) and generously funded by the Donna and Benjamin Rosen Bioengineering Center at Caltech. Finally and sadly, since the completion of this chapter, my friend and collaborator Bill Klug was brutally murdered in his office by a former graduate student. I had asked Bill to join me in the writing of this chapter, but he was too busy during this summer and instead of having the happy presence of his name as a co-author I instead have the solemn and unhappy duty to dedicate this short piece to him, kind and intellectually deep, above all a family man, he will be deeply missed.

References

1. Buehler LK (2016) Cell membranes. Garland Press, New York
2. Milo R, Jorgensen P, Moran U, Weber G, Springer M (2010) BioNumbers—the database of key numbers in molecular and cell biology. Nucleic Acids Res 38:D750–D753
3. Mahajan S (2014) The art of insight in science and engineering: mastering complexity. The MIT Press, Cambridge
4. Phillips R, Kondev J, Theriot J, Garcia HG (2013) Physical biology of the cell, 2nd edn. Garland Science, New York. Illustrated by N. Orme
5. Tanford C (2004) Ben Franklin stilled the waves. Oxford University Press, New York
6. Pockels A (1891) Surface tension. Nature 43:437–439
7. Langmuir I (1917) The constitution and fundamental properties of solids and liquids. II. Liquids. J Am Chem Soc 39:1848–1906
8. Gorter E, Grendel F (1925) On bimolecular layers of lipoids on the chromocytes of the blood. J Exp Med 41:439–443

9. Nagle JF, Tristram-Nagle S (2000) Structure of lipid bilayers. Biochim Biophys Acta 1469:159–195
10. Nagle JF, Zeidel ML, Mathai JC, Tristram-Nagle S (2008) Structural determinants of water permeability through the lipid membrane. J Gen Physiol 131:69–76
11. Boal D (2002) Mechanics of the cell, 1st edn. Cambridge University Press, Cambridge
12. Harroun TA, Weiss TM, Yang L, Huang HW (1999) Theoretical analysis of hydrophobic matching and membrane-mediated interactions in lipid bilayers containing gramicidin. Biophys J 76(6):3176–3185
13. Nielsen C, Andersen OS (2000) Inclusion-induced bilayer deformations: effects of monolayer equilibrium curvature. Biophys J 79(5):2583–2604
14. Phillips R, Ursell T, Wiggins P, Sens P (2009) Emerging roles for lipids in shaping membrane-protein function. Nature 459(7245):379–385
15. Neupert W (2012) SnapShot: mitochondrial architecture. Cell 149(3):722–722.e1
16. Shibata Y, Voeltz GK, Rapoport TA (2006) Rough sheets and smooth tubules. Cell 126(3): 435–439
17. Shibata Y, Shemesh T, Prinz WA, Palazzo AF, Kozlov MM, Rapoport TA (2010) Mechanisms determining the morphology of the peripheral ER. Cell 143(5):774–788
18. Takamori S, Holt M, Stenius K, Lemke EA, Gronborg M, Riedel D, Urlaub H, Schenck S, Brugger B, Ringler P, Muller SA, Rammner B, Grater F, Hub JS, De Groot BL, Mieskes G, Moriyama Y, Klingauf J, Grubmuller H, Heuser J, Wieland F, Jahn R (2006) Molecular anatomy of a trafficking organelle. Cell 127(4):831–846
19. Milo R, Phillips R (2016) Cell biology by the numbers. Garland Press, New York
20. Dupuy AD, Engelman DM (2008) Protein area occupancy at the center of the red blood cell membrane. Proc Natl Acad Sci U S A 105(8):2848–2852
21. van Meer G, Voelker DR, Feigenson GW (2008) Membrane lipids: where they are and how they behave. Nat Rev Mol Cell Biol 9(2):112–124
22. Ejsing CS, Sampaio JL, Surendranath V, Duchoslav E, Ekroos K, Klemm RW, Simons K, Shevchenko A (2009) Global analysis of the yeast lipidome by quantitative shotgun mass spectrometry. Proc Natl Acad Sci U S A 106(7):2136–2141
23. Kalvodova L, Sampaio JL, Cordo S, Ejsing CS, Shevchenko A, Simons K (2009) The lipidomes of vesicular stomatitis virus, semliki forest virus, and the host plasma membrane analyzed by quantitative shotgun mass spectrometry. J Virol 83(16):7996–8003
24. Sampaio JL, Gerl MJ, Klose C, Ejsing CS, Beug H, Simons K, Shevchenko A (2011) Membrane lipidome of an epithelial cell line. Proc Natl Acad Sci U S A 108(5):1903–1907
25. Layre E, Sweet L, Hong S, Madigan CA, Desjardins D, Young DC, Cheng TY, Armand JW, Kim K, Shamputa IC, McConnell MJ, Debono CA, Behar SM, Minnaard AJ, Murray M, Barry CE, Matsunaga I, Moody DB (2011) A comparative lipidomics platform for chemotaxonomic analysis of mycobacterium tuberculosis. Chem Biol 18:1537–1549
26. Carvalho M, Sampaio JL, Palm W, Brankatschk M, Eaton S, Shevchenko A (2012) Effects of diet and development on the *Drosophila* lipidome. Mol Syst Biol 8:600
27. Klose C, Surma MA, Gerl MJ, Meyenhofer F, Shevchenko A, Simons K (2012) Flexibility of a eukaryotic lipidome–insights from yeast lipidomics. PLoS One 7(4):e35063
28. Klose C, Surma MA, Simons K (2013) Organellar lipidomics–background and perspectives. Curr Opin Cell Biol 25(4):406–413
29. Neidhardt FC, Ingraham JL, Schaechter M (1990) Physiology of the bacterial cell: a molecular approach. Sinauer Associates, Sunderland
30. Levental KR, Levental I (2015) Giant plasma membrane vesicles: models for understanding membrane organization. Curr Top Membr 75:25–57
31. Evans E, Rawicz W, Smith BA (2013) Back to the future: mechanics and thermodynamics of lipid biomembranes. Faraday Discuss 161:591–611
32. Rawicz W, Olbrich KC, McIntosh T, Needham D, Evans E (2000) Effect of chain length and unsaturation on elasticity of lipid bilayers. Biophys J 79(1):328–339
33. Nagle JF, Jablin MS, Tristram-Nagle S, Akabori A (2015) What are the true values of the bending modulus of simple lipid bilayers? Chem Phys Lipids 185:3–10

34. Song J, Waugh RE (1993) Bending rigidity of SOPC membranes containing cholesterol. Biophys J 64:1967–1970
35. Hochmuth FM, Shao JY, Dai J, Sheetz MP (1996) Deformation and flow of membrane into tethers extracted from neuronal growth cones. Biophys J 70(1):358–369
36. Dai J, Sheetz MP, Wan X, Morris CE (1998) Membrane tension in swelling and shrinking molluscan neurons. J Neurosci 18(17):6681–6692
37. Olbrich KC, Rawicz W, Needham D, Evans E (2000) Water permeability and mechanical strength of polyunsaturated lipid bilayers. Biophys J 79:321–327
38. Upadhyaya A, Sheetz MP (2004) Tension in tubulovesicular networks of Golgi and endoplasmic reticulum membranes. Biophys J 86(5):2923–2928
39. Peukes J, Betz T (2014) Direct measurement of the cortical tension during the growth of membrane blebs. Biophys J 107(8):1810–1820
40. Sens P, Plastino J (2015) Membrane tension and cytoskeleton organization in cell motility. J Phys Condens Matter 27(27):273103
41. Kedem O, Katchalsky A (1958) Thermodynamic analysis of the permeability of biological membranes to non-electrolytes. Biochim Biophys Acta 27:229–246
42. Manning GS (1968) Binary diffusion and bulk flow through a potential-energy profile: a kinetic basis for the thermodynamic equations of flow through membranes. J Chem Phys 49: 2668–2675
43. Robinett RW (2015) Dimensional analysis as the other language of physics. Am J Phys 83: 353–361
44. Finkelstein A (1976) Water and nonelectrolyte permeability of lipid bilayer membranes. J Gen Physiol 68(2):127–135
45. Stein WD (1990) Channels, carriers and pumps. An introduction to membrane transport. Academic, Cambridge
46. Schlessinger J, Axelrod D, Koppel DE, Webb WW, Elson EL (1977) Lateral transport of a lipid probe and labeled proteins on a cell membrane. Science 195(4275):307–309
47. Alecio MR, Golan DE, Veatch WR, Rando RR (1982) Use of a fluorescent cholesterol derivative to measure lateral mobility of cholesterol in membranes. Proc Natl Acad Sci U S A 79(17):5171–5174
48. Gaede HC, Gawrisch K (2003) Lateral diffusion rates of lipid, water, and a hydrophobic drug in a multilamellar liposome. Biophys J 85(3):1734–1740
49. Doeven MK, Folgering JH, Krasnikov V, Geertsma ER, van den Bogaart G, Poolman B (2005) Distribution, lateral mobility and function of membrane proteins incorporated into giant unilamellar vesicles. Biophys J 88(2):1134–1142
50. Nenninger A, Mastroianni G, Robson A, Lenn T, Xue Q, Leake MC, Mullineaux CW (2014) Independent mobility of proteins and lipids in the plasma membrane of *Escherichia coli*. Mol Microbiol 92(5):1142–1153
51. Fahey PF, Koppel DE, Barak LS, Wolf DE, Elson EL, Webb WW (1977) Lateral diffusion in planar lipid bilayers. Science 195(4275):305–306
52. Saffman PG, Delbruck M (1975) Brownian motion in biological membranes. Proc Natl Acad Sci U S A 72(8):3111–3113
53. Gambin Y, Lopez-Esparza R, Reffay M, Sierecki E, Gov NS, Genest M, Hodges RS, Urbach W (2006) Lateral mobility of proteins in liquid membranes revisited. Proc Natl Acad Sci U S A 103(7):2098–2102
54. Ramadurai S, Holt A, Krasnikov V, van den Bogaart G, Killian JA, Poolman B (2009) Lateral diffusion of membrane proteins. J Am Chem Soc 131(35):12650–12656
55. Kumar M, Mommer MS, Sourjik V (2010) Mobility of cytoplasmic, membrane, and DNA-binding proteins in *Escherichia coli*. Biophys J 98(4):552–559
56. Chow D, Guo L, Gai F, Goulian M (2012) Fluorescence correlation spectroscopy measurements of the membrane protein TetA in *Escherichia coli* suggest rapid diffusion at short length scales. PLoS One 7(10):e48600
57. Mika JT, Schavemaker PE, Krasnikov V, Poolman B (2014) Impact of osmotic stress on protein diffusion in *Lactococcus lactis*. Mol Microbiol 94(4):857–870

58. Hanai T, Haydon DA, Taylor J (1965) The variation of capacitance and conductance of bimolecular lipid membranes with area. J Theor Biol 9:433–443
59. Vorobyov I, Olson TE, Kim JH, Koeppe RE 2nd, Andersen OS, Allen TW (2014) Ion-induced defect permeation of lipid membranes. Biophys J 106(3):586–597
60. Haswell ES, Phillips R, Rees DC (2011) Mechanosensitive channels: what can they do and how do they do it? Structure 19(10):1356–1369
61. Fricke H (1925) The electric capacity of suspensions with special reference to blood. J Gen Physiol 9:137–152
62. Curtis HJ, Cole KS (1938) Transverse electric impedance of the squid giant axon. J Gen Physiol 21:757–765
63. Almers W (1978) Gating currents and charge movements in excitable membranes. Rev Physiol Biochem Pharmacol 82:97–190
64. Fagerberg L, Jonasson K, von Heijne G, Uhlen M, Berglund L (2010) Prediction of the human membrane proteome. Proteomics 10(6):1141–1149
65. Li GW, Burkhardt D, Gross C, Weissman JS (2014) Quantifying absolute protein synthesis rates reveals principles underlying allocation of cellular resources. Cell 157(3):624–635
66. Schmidt A, Kochanowski K, Vedelaar S, Ahrne E, Volkmer B, Callipo L, Knoops K, Bauer M, Aebersold R, Heinemann M (2016) The quantitative and condition-dependent *Escherichia coli* proteome. Nat Biotechnol 34(1):104–110
67. Li M, Hazelbauer GL (2004) Cellular stoichiometry of the components of the chemotaxis signaling complex. J Bacteriol 186(12):3687–3694
68. Bitbol AF, Wingreen NS (2015) Fundamental constraints on the abundances of chemotaxis proteins. Biophys J 108(5):1293–1305
69. Bialecka-Fornal M, Lee HJ, Phillips R (2015) The rate of osmotic downshock determines the survival probability of bacterial mechanosensitive channel mutants. J Bacteriol 197(1): 231–237
70. Louhivuori M, Jelger Risselada H, van der Giessen E, Marrink SJ (2010) Release of content through mechano-sensitive gates in pressurized liposomes. Proc Natl Acad Sci U S A 107: 19856–19860
71. Andersen OS (1983) Ion movement through gramicidin a channels single-channel measurements at very high potentials. Biophys J 41:119–133
72. Bintu L, Buchler NE, Garcia HG, Gerland U, Hwa T, Kondev J, Phillips R (2005) Transcriptional regulation by the numbers: models. Curr Opin Genet Dev 15(2):116–124
73. Garcia HG, Sanchez A, Kuhlman T, Kondev J, Phillips R (2010) Transcription by the numbers redux: experiments and calculations that surprise. Trends Cell Biol 20:723–733
74. Phillips R, Milo R (2009) A feeling for the numbers in biology. Proc Natl Acad Sci U S A 106(51):21465–21471
75. Moran U, Phillips R, Milo R (2010) SnapShot: key numbers in biology. Cell 141(7): 1262–1262.e1
76. Flamholz A, Phillips R, Milo R (2014) The quantified cell. Mol Biol Cell 25(22):3497–3500
77. Shamir M, Bar-On Y, Phillips R, Milo R (2016) SnapShot: timescales in cell biology. Cell 164(6):1302–1302.e1
78. Phillips R (2015) Theory in biology: Figure 1 or Figure 7? Trends Cell Biol 25(12):723–729
79. Bialek W (2015) Perspectives on theory at the interface of physics and biology. ArXiv: 1512.08954
80. Seifert U (1997) Configurations of fluid membranes and vesicles. Adv Phys 46:13
81. Savin T, Kurpios NA, Shyer AE, Florescu P, Liang H, Mahadevan L, Tabin CJ (2011) On the growth and form of the gut. Nature 476(7358):57–62
82. Shyer AE, Tallinen T, Nerurkar NL, Wei Z, Gil ES, Kaplan DL, Tabin CJ, Mahadevan L (2013) Villification: how the gut gets its villi. Science 342(6155):212–218
83. Dacks JB, Peden AA, Field MC (2009) Evolution of specificity in the eukaryotic endomembrane system. Int J Biochem Cell Biol 41(2):330–340

84. Field MC, Dacks JB (2009) First and last ancestors: reconstructing evolution of the endomembrane system with ESCRTs, vesicle coat proteins, and nuclear pore complexes. Curr Opin Cell Biol 21(1):4–13
85. Richardson E, Zerr K, Tsaousis A, Dorrell RG, Dacks JB (2015) Evolutionary cell biology: functional insight from "endless forms most beautiful". Mol Biol Cell 26:4532–4538